Nephrol Dial Transplant (1999) 14: 2860–2872

Nephrology
Dialysis
Transplantation

Original Article

Glomerular epithelial–myofibroblast transdifferentiation in the evolution of glomerular crescent formation

Yee-Yung Ng[1], Jun-Ming Fan[2], Wei Mu[2], David J. Nikolic-Paterson[2], Wu-Chang Yang[1], Tung-Po Huang[1], Robert C. Atkins[2] and Hui Y. Lan[2]

[1]Department of Nephrology, Veterans General Hospital-Taipei, National Yang-Ming University, Taipei, Taiwan and
[2]Departments of Nephrology and Medicine, Monash Medical Centre, Monash University, Clayton, Victoria, Australia

Abstract

Background. Glomerular cellular crescents consist of epithelial cells and macrophages, which can undergo an irreversible process of fibrous organization. However, the origin of the fibroblast-type cells that mediate this fibrous organization is unclear.

Methods. This study examined glomerular epithelial–myofibroblast transdi erentiation (GEMT) in the formation and evolution of glomerular crescents in two distinct rat models of glomerulonephritis: 5/6 nephrectomy and antiglomerular basement membrane (GBM) disease.

Results. Early in the course of both disease models, and prior to crescent formation, immunohistochemistry staining and in-situ hybridization demonstrated de novo expression of alpha-smooth-muscle actin (α-SMA), a marker of smooth muscle cells and myofibroblasts, by glomerular parietal epithelial cells (GPEC). The expression of α-SMA by GPEC was accompanied by a loss of E-cadherin staining, a marker of epithelial cells. At this early stage of GEMT, ultrastructural studies identified the presence of characteristic actin microfilaments and dense bodies within GPEC which retained a normal epithelial morphology with apical-basal polarity and microvilli. A late stage of transdi erentiation was seen in fibrocellular crescents. In this case, GPEC attached to intact segments of the capsular basement membrane contained large bundles of actin microfilaments throughout the cell, and this was accompanied by a loss of polarity, microvilli, and tight junctions. There was a significant correlation between the presence of α-SMA$^+$ GPEC and glomerular crescent formation. Cellular crescents contained small numbers of α-SMA$^+$ myofibroblasts. These cells become the dominant population in fibrocellular crescents, which was associated with marked local proliferation. Relatively few α-SMA$^+$ myofibroblasts remained in fibrotic/organizing crescents. Most cells within cellular and fibrocellular crescents expressed transforming growth factor-β (TGF-β) and basic fibroblast growth factor (FGF-2), suggesting that these growth factors may regulate this GEMT process during the evolution of glomerular crescents.

Conclusions. This study provides the first phenotypic and morphological evidence that glomerular epithelial-myofibroblast transdi erentiation participates in the formation and evolution of glomerular crescents.

Key words: glomerular crescents; glomerular epithelial cells; glomerulonephritis; myofibroblasts; transdi erentiation

Introduction

Glomerular crescent formation is a feature of rapidly progressive glomerulonephritis, indicating severe glomerular damage, and providing a useful diagnostic and prognostic marker of disease progression [1]. There are three distinct stages of glomerular crescent formation. Cellular crescents comprise proliferating epithelial cells, macrophages, or a mixture of the two cell types, depending upon the nature of the glomerular injury [2–7]. In some circumstances cellular crescents, particularly those of a predominantly epithelial morphology, can resolve [reviewed in 8]. A key step in the irreversible fibrous organization of cellular crescents is disruption of the capsular basement membrane (CBM). This allows the entry of periglomerular fibroblasts and leukocytes into the Bowman's space, leading to the formation of a fibrocellular crescent which progresses to become an acellular fibrous crescent [5,9–11].

Although fibroblasts play a crucial role in the fibrous organization of cellular crescents, the nature of these cells and their origins is not clear. The expression of α-smooth-muscle actin (α-SMA) has been used as a marker of myofibroblasts, a subset of fibroblasts, which are a major source of collagen synthesis [12–14]. Indeed, increasing numbers of interstitial α-SMA$^+$ myofibroblasts predicts progressive renal dysfunction

Correspondence and offprint requests to: Dr Hui Y. Lan, Department of Nephrology, Monash Medical Centre, Clayton Road, Clayton, Victoria 3168, Australia.

in human and experimental glomerulonephritis [15–20]. However, the potential role of α-SMA$^+$ myofibroblasts in the formation and progression of glomerular crescents has not been examined.

It has been postulated that the accumulation of fibroblasts in glomerular crescents arises from the entry of periglomerular fibroblasts through the ruptured CBM [5,9–11]. However, the growing appreciation of the ability of epithelial cells to undergo transdi erentiation into mesenchymal cells, and α-SMA$^+$ myofibroblasts in particular, has led us to re-evaluate the possible origins of fibroblast-like cells within glomerular crescents.

The aim of the current study was therefore to examine the origins and contribution of myofibroblasts in the formation and evolution of glomerular crescents. This was performed in two contrasting experimental models of crescentic glomerulonephritis; non-immune renal ablation and immune-induced antiglomerular basement membrane (GBM) glomerulonephritis.

Subjects and methods

Non-immune model of crescentic glomerulonephritis

The 5/6-nephrectomy model of glomerulonephritis followed a previously described protocol [21]. Male Sprague–Dawley rats (150–200 g) were obtained from the Central Animal House, Yang Ming University, Taiwan. Thirty-six animals underwent subtotal nephrectomy involving right subcapsular nephrectomy and infarction of approximately two-thirds of the left kidney by ligation of the posterior and one or two anterior extrarenal branches of renal artery. After the surgery, rats were randomly assigned into groups of six animals, which were sacrificed at weeks 1, 3, 5, 9, 13, and 17. As a control, a second set of 36 rats underwent a sham operation consisting of laparotomy and manipulation of the renal pedicles but without damage to the kidney. Groups of six animals were sacrificed at the same time points as described above. A group of six normal rats was used as a control.

Immune model of crescentic glomerulonephritis

Male Sprague–Dawley rats (150–200 g) were obtained from the Monash Animal Services, Melbourne. Experimental crescentic glomerulonephritis was induced as previously described [22]. Briefly, animals were immunized s.c. with 5 mg normal rabbit IgG in Freund's complete adjuvant and injected i.v. with 10 ml/kg body weight rabbit anti-rat GBM serum (12.5 mg IgG/ml) 5 days later (termed day 0). Groups of six animals were killed on days 1, 7, 14, 21, and 35. In addition, a group of six normal animals was used as a control.

Histopathology

Kidney tissues for histological examination were fixed in 10% formalin and 4 μm para n sections were stained with haematoxylin and eosin or periodic acid–Schi reagent (PAS). Glomerular crescent formation was scored as previously described [6,11]. Briefly, the percentage of glomeruli with crescent formation was assessed by examining 50–100 glomeruli per animal on PAS-stained para n-sections, and glomerular crescents were classified into three categories as follow: (i) cellular crescents containing three or more layers of cells, with most cells having a round morphology; (ii) fibrocellular crescents, defined as cellular crescents containing fibroblasts and some collagen; and (iii) fibrous/sclerotic crescents having fibrous appearance with few cells. The integrity of the basement membrane of Bowman's capsule was assessed on PAS-stained para n-sections.

Antibodies

Monoclonal antibodies (mAb) used were: 1A4, which specifically recognized the smooth-muscle α-actin isoform expressed by rat, mouse and human (Sigma Chemical Co., St Louis, MO); PC10, mouse anti-proliferating cell nuclear antigen (PCNA) which is expressed by cells in G1, S, and G2 phases of the cell cycle (Dakopatts, Glostrup, Denmark); ED1, mouse anti-rat macrophages [23]; OX-7, mouse anti-rat Thy-1 antigen [24]; mouse anti-bovine FGF-2 which cross-reacts with rat FGF-2 but does not recognize bovine or rat FGF-1 (Upstate Biotechnology Inc., Lake Placid, NY); mouse anti-rat E-cadherin (Transduction Laboratories, Lexington, KY); rabbit anti-human transforming growth factor betα-1 (TGF-β1) which cross-reacts with rat TGF-β1 but does not react with other TGF-β subclasses (Santa Cruz, CA). In addition, peroxidase-conjugated goat anti-mouse IgG, colloidal gold conjugated goat anti-mouse IgG, alkaline phosphatase-conjugated goat anti-mouse IgG, mouse peroxidase anti-peroxidase complexes (PAP) and mouse alkaline phosphatase anti-alkaline phosphatase complexes (APAAP) were purchased from Dakopatts.

Immunohistochemistry

Double immunohistochemistry was performed using a microwave-based two-colour staining technique [25]. Briefly, sections were dewaxed, pre-incubated for 20 min in 10% FCS and 10% normal goat serum to block non-specific binding, incubated with the anti-α-SMA or anti-E-cadherin mAb for 60 min and washed three times in phosphate-bu ered saline (PBS). After inactivating endogenous peroxidase in 0.3% H2O2 in methanol, sections were labelled sequentially with peroxidase-conjugated goat anti-mouse IgG and PAP, followed by development with diaminobenzidine to produce a brown colour. To block antibody cross-reactivity and facilitate antigen retrieval [25], sections were treated with 2×5 min of microwave oven heating in 10 mM sodium citrate pH 6.0 at 2450 MHz and 800 W power. Sections were then pre-incubated as above, incubated with the PC-10 (1 : 1000) or anti-α-SMA mAb for 60 min, followed by alkaline-phosphatase-conjugated goat anti-mouse IgG and APAAP, and finally developed with Fast Blue BB Base (Sigma Chemical Co.), counterstained with PAS without haematoxylin, and coverslipped in an aqueous mounting medium. Negative controls consisted of substitution of one or both of the primary antibodies with an equivalent concentration of an irrelevant murine monoclonal antibody (73.5, anti-human CD45R). All procedures were performed at room temperature.

Triple immunostaining was performed as described previously [26]. First, sections were stained with the anti-FGF-2 mAb using a three-layer PAP method to produce a brown colour. Second, sections were microwaved and then stained with the ED1 mAb using a three-layer APAAP method to produce a blue colour. Third, sections were microwaved again and then stained with the PC-10 mAb

followed by colloidal gold-conjugated goat anti-mouse IgG and silver enhancement to produce a black colour.

Immunostaining for the Thy-1 antigen using the OX-7 mAb was performed on ethanol-fixed, snap frozen tissues using a three-layer PAP method as described above.

Quantitation of immunohistochemical staining

The total number of nucleated cells and the number of α-SMA$^+$, PCNA$^+$, α-SMA$^+$PCNA$^+$, and α-SMA$^+$PCNA$^-$ cells within glomerular crescents were scored in double-stained sections as previously described [6,26]. At least 10 glomerular crescent cross-sections of cellular, fibrocellular, and fibrous crescents (if present) were scored for each animal in high-power fields ($\times 40$). In addition, glomerular parietal epithelial cells were examined by scoring cross-sections of Bowman's space in glomeruli without crescent formation. The total number of nucleated cells and the number of nucleated α-SMA$^+$, PCNA$^+$, α-SMA$^+$PCNA$^+$, and α-SMA$^+$PCNA$^-$ cells were scored in at least 50 Bowman's space cross-sections per animal. Data from groups of six animals is expressed as the mean $\pm$ standard error of the mean (SEM) per Bowman's space cross-section or per crescent cross-section. For all morphological analyses, the observer was blinded to the animal group.

Probes

A 1068 base pair cDNA fragment of rat vascular smooth-muscle α-actin [27], and a 980 base pair cDNA fragment of rat transforming growth factor-β1 [28], were amplified by the polymerase chain reaction and cloned using the pMOSBlue T-vector kit (Amersham International, Buckinghamshire, UK). A 180 base pair cDNA fragment of rat FGF-2 cloned into pGEM3Zf was a gift from Dr Miriam Ford, University of Melbourne. Both sense and anti-sense digoxigenin (DIG)-labelled cRNA probes were prepared using an RNA polymerase kit (Boehringer Mannheim GmbH, Mannheim, Germany). Probes were precipitated and incorporation of DIG was determined by dot blotting.

In situ *hybridization*

In situ hybridization was performed on 4 μm para n sections of formalin-fixed tissue using a microwave-based protocol [26,29]. After dewaxing, sections were treated with a microwave oven for 2×5 min as described above, incubated with 0.2 M HCl for 15 min, followed by 1% Triton X-I00 for 15 min, and then digested for 20 min with 10 μg/ml Proteinase-K at 37°C (Boehringer Mannheim). Sections were then washed in $2 \times$ SSC, prehybridized, and then hybridized with 0.3 ng/μl DIG-labelled sense or anti-sense α-SMA, TGF-β, or FGF-2 cRNA probe overnight at 37°C in a hybridization bu er containing 50% deionized formamide, $4 \times$ SSC, $2 \times$ Denhardt's solution, 1 mg/ml salmon sperm DNA, and 1 mg/ml yeast tRNA. Sections were finally washed in $0.1 \times$ SSC at 37°C and the hybridized probe detected using sheep anti-DIG antibody (Fab) conjugated with alkaline phosphatase and colour development with NBT/X-phosphate (Boehringer Mannheim). No signal was seen with the sense riboprobe labelled to the same specific activity.

As another specificity control, some sections were microwave treated after hybridization with the anti-sense α-SMA cRNA probe and then stained with the anti-α-SMA mAb using the three-layer APAAP method as described above. All sections were counterstained with PAS minus haematoxylin and mounted in an aqueous medium.

In addition, some sections hybridized with the anti-sense TGF-β1 cRNA probe were subsequently stained with the anti-α-SMA mAb using a threelayer APAAP method to produce a blue colour.

Electron microscopy

Small tissue blocks obtained from the renal cortex were fixed in 2.5% glutaraldehyde in PBS (pH 7.4) for 4 h, washed in PBS, post-fixed with 1% osmium tetroxide, dehydrated in graded alcohol, and embedded in Epon 812. Ultrathin sections were stained with uranyl acetate and lead citrate and examined in under a Zeiss electron microscope (EMIOC).

Statistical analysis

Di erences in the number of labelled cells counted in tissue sections were analysed by one-way analysis of variance (ANOVA) from the Complete Statistical Analysis program (CSS, Statsoft, Tulsa, IL, USA). In addition, the number of labelled cells scored in tissue sections was correlated with crescent formation using the Pearson single correlation coe cient.

Results

α-SMA expression in normal and sham-operated rat kidney

Expression of α-SMA was used as a phenotypic marker of myofibroblasts. In normal and sham-operated rats, α-SMA mRNA and protein was readily observed in vascular smooth-muscle cells and occasional interstitial cells, but was absent from glomerular, cortical, and medullary epithelial cells (Figures 1a and 2a). On the basis of expression of the proliferating cell nuclear antigen (PCNA), few cells in the tubulointerstitial or glomerular compartments of normal or sham-operated rats showed evidence of proliferation (Figure 2a). Virtually all renal epithelial cells, including glomerular visceral and parietal epithelial cells, expressed the epithelial marker, E-cadherin (Figure 3a). Of note, both parietal and visceral epithelial cells expressed vimentin, making this an unsuitable marker for identifying glomerular epithelial–mesenchymal trans-di erentiation.

Phenotypic evidence for glomerular epithelial–myofibroblast transdifferentiation (GEMT) in the initiation of glomerular crescent formation

In the early stages of renal disease following 5/6 nephrectomy (weeks 1–3), de novo expression of α-SMA mRNA by some glomerular parietal epithelial cells (GPEC), and to a lesser extent by some glomerular visceral epithelial cells, was detected (Figure 1b).

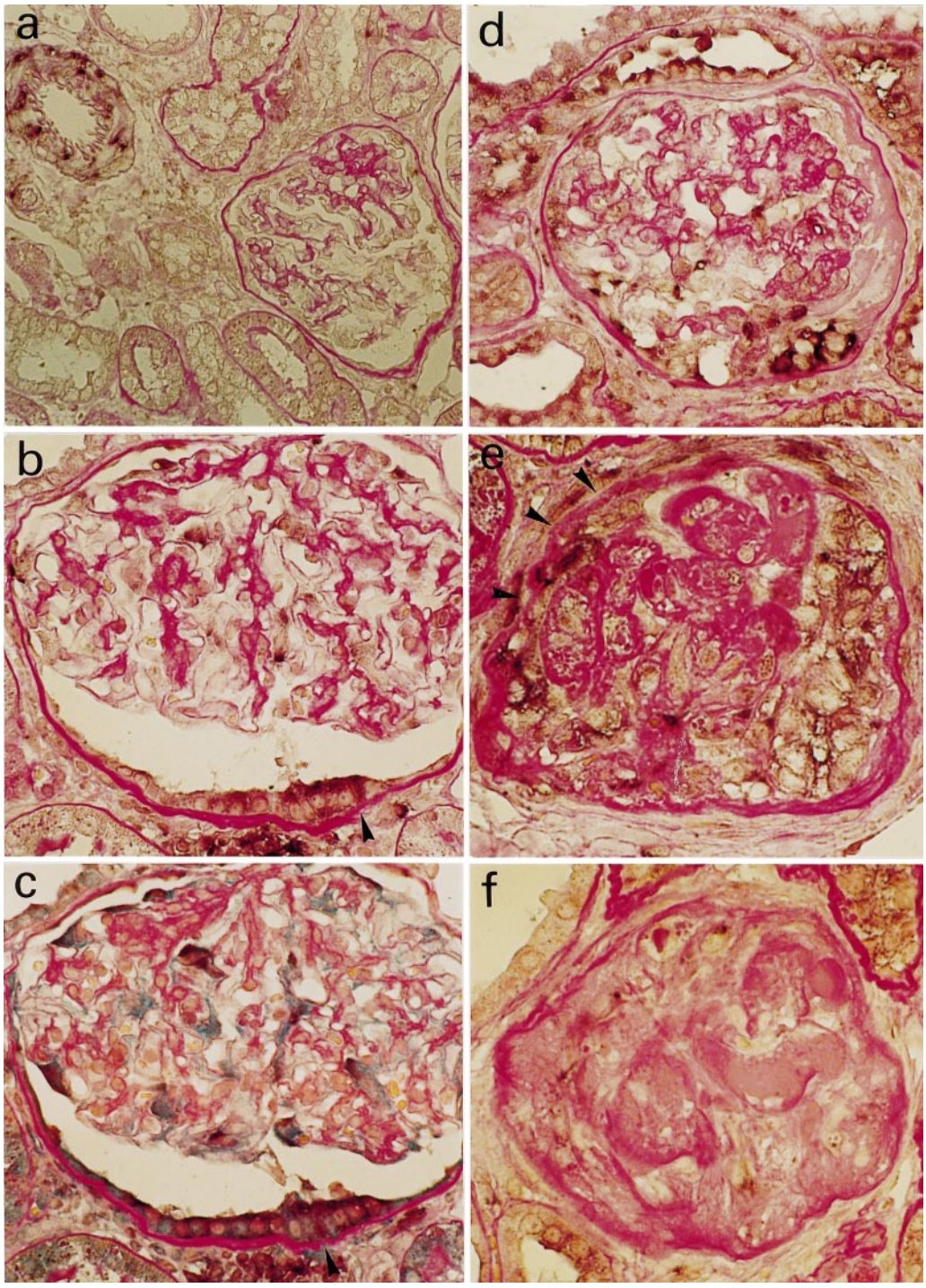

Fig. 1a–f. *In-situ* hybridization demonstrating α-SMA mRNA expression by GEC during glomerular crescent formation and progression in the rat remnant kidney and anti-GBM glomerulonephritis. (**a**) Normal animal showing strong α-SMA mRNA expression (purple) in vascular smooth-muscle cells, but no signal is seen in tubules or glomeruli. (**b**) *De-novo* expression of α-SMA mRNA (purple) by glomerular visceral and parietal epithelial cells in the early stage of GEMT in a week 3 nephrectomized rat. Note the early transformed GEC with normal epithelial morphology and the partial disruption of the CBM (arrowhead). (**c**) Serial section of (b) showing strong co-expression of α-SMA mRNA (purple) and α-SMA protein (blue) by the transformed GEC demonstrated by double *in-situ* hybridization and immunostaining. (**d**) Strong α-SMA mRNA expression within a glomerular cellular crescent at week 5 remnant kidney. (**e**) Strong α-SMA mRNA expression within a fibrocellular crescent at day 21 of anti-GBM glomerulonephritis. Note the CBM is thickened and wrinkled with partial and extensive disruption (arrowheads) and many α-SMA mRNA$^+$ myofibroblasts have accumulated in the periglomerular area. (**f**) A fibrous crescent showing few α-SMA$^+$ mRNA cells. All sections were counterstained with PAS (pink). ×100 (a), ×250 (b–f).

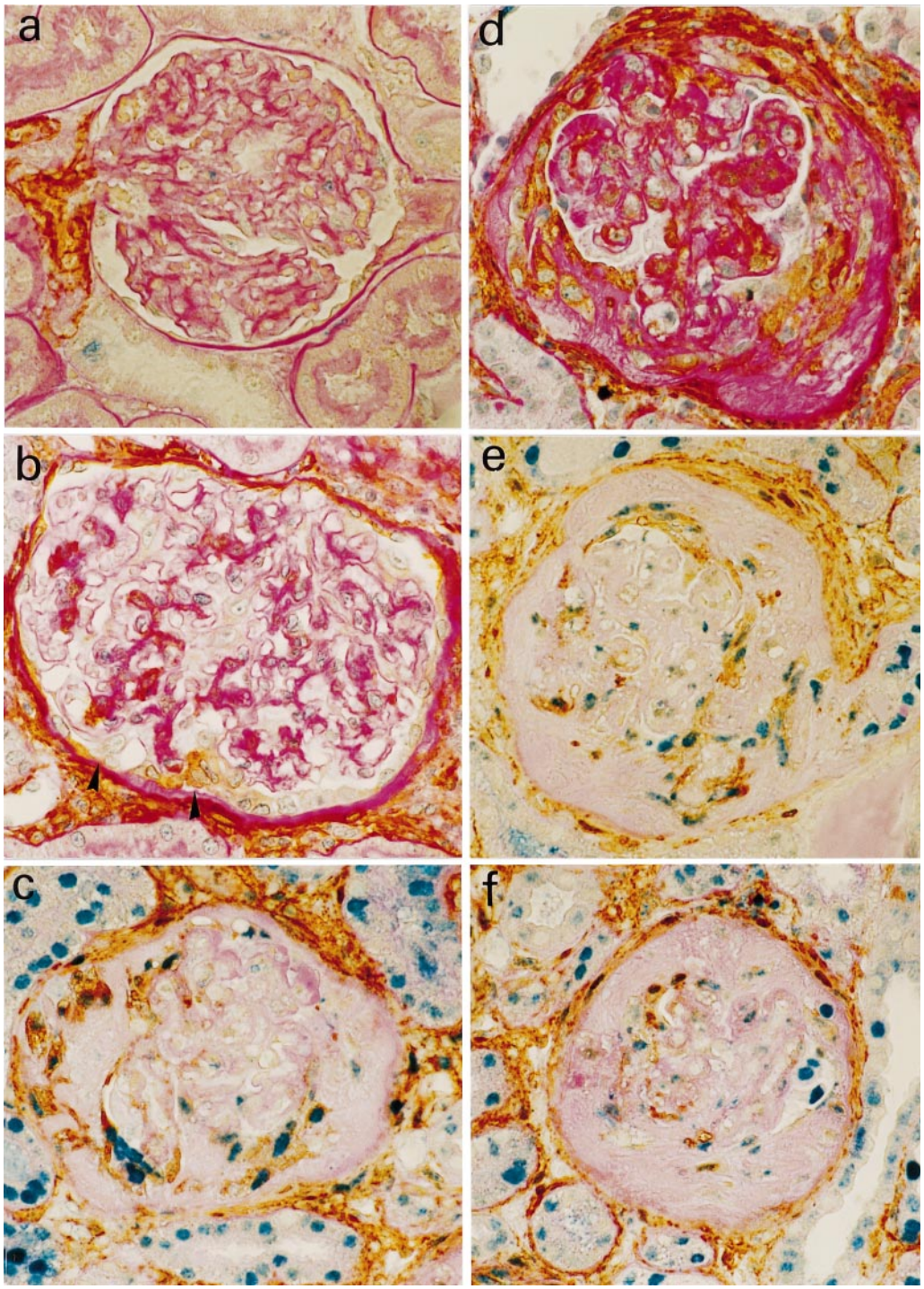

Fig. 2a–f. Double immunohistochemistry demonstrating glomerular epithelial cell proliferation and myofibroblast transdi erentiation in the rat remnant kidney and anti-GBM glomerulonephritis. All sections are stained for α-SMA protein (brown), and sections (a,c,e,f) are double stained for PCNA (blue nuclei). (**a**) Normal rat kidney showing normal histology with occasional proliferating $PCNA^+$ cells and α-SMA staining limited to vessels. (**b**) Day 7 anti-GBM glomerulonephritis showing early stage of GEMT. Individual and small clusters of transformed GPEC expressing α-SMA are seen within Bowman's space. The transformed GPEC partly retain apical–basal polarity and the CBM is partially disrupted (arrowhead). (**c**) Strong α-SMA expression within a cellular crescent at day 14 of anti-GBM glomerulonephritis. Note that most $\alpha\text{-SMA}^+$ cells are proliferating ($PCNA^+$). (**d**) Week 17 in the remnant kidney showing many $\alpha\text{-SMA}^+$ myofibroblasts with elongated morphology within a fibrocellular crescent. The CBM is extensively damaged. (**e**) An advanced fibroellular crescent at day 21 of anti-GBM glomerulonephritis. Many $\alpha\text{-SMA}^+$ myofibroblasts are proliferating. Note abundant collagen within the crescent and complete disruption of CBM where numerous $\alpha\text{-SMA}^+$ myofibroblasts have accumulated. (**f**) A fibrous crescent at day 35 of anti-GBM glomerulonephritis showing a few proliferating $\alpha\text{-SMA}^+$ myofibroblasts within a collagen-rich sclerotic crescent. The CBM is completely disrupyed. All sections were counterstained with PAS (pink). ×250.

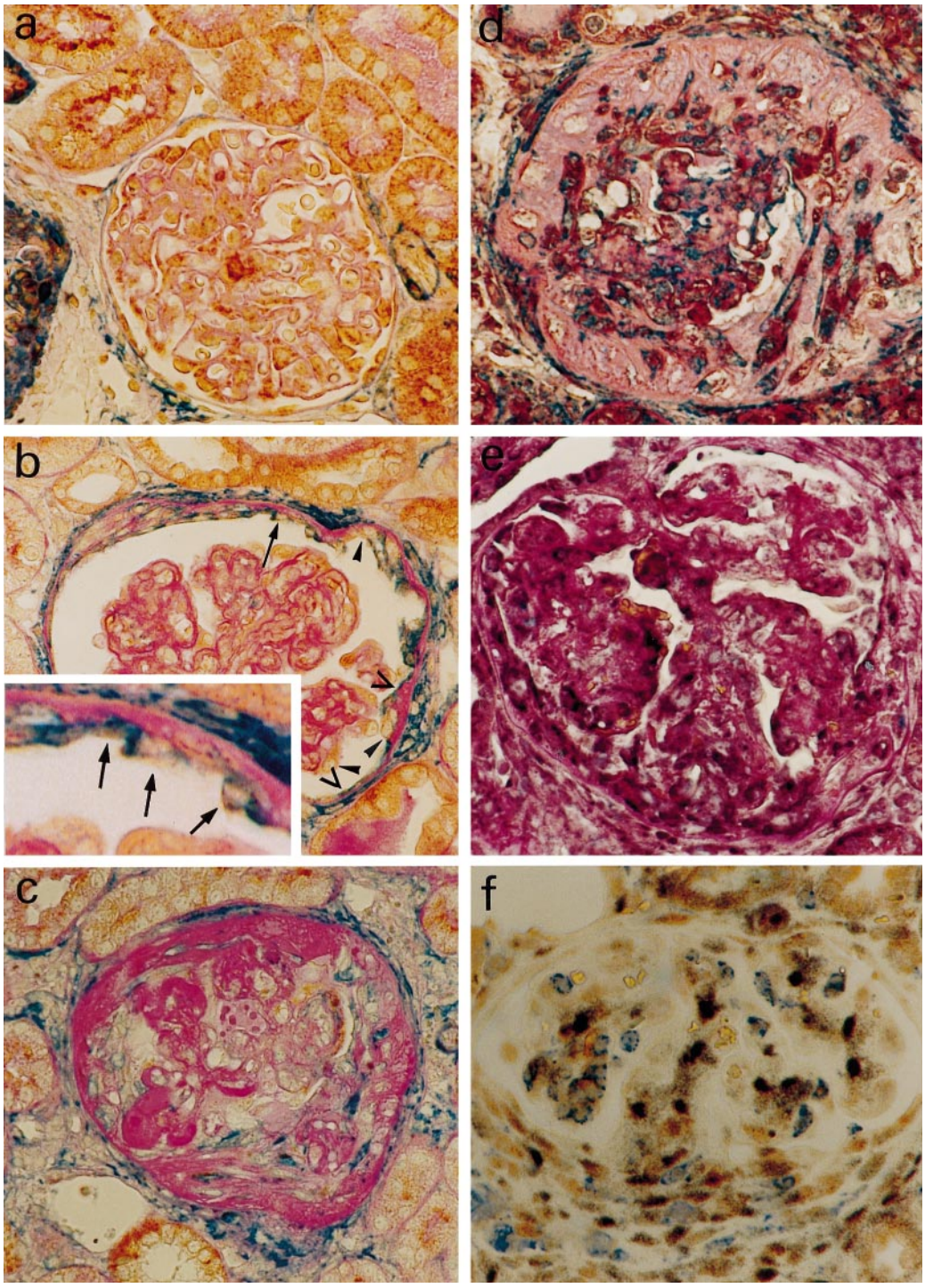

Fig. 3a–f. Double immunohistochemistry and *in-situ* hybridization demonstration of E-cadherin, TGF-β and FGF-2 expression by GPEC during glomerular crescent formation and progression in anti-GBM glomerulonephritis. (**a**) Normal rat kidney showing E-cadhrin expression by both glomerular and tubular epithelial cells (brown), while α-SMA expression was limited to vascular smooth muscle and some interstitial myofibroblasts (blue). (**b**) An early stage of GEMT at day 7 anti-GBM glomerulonephritis. Early transformed GPEC can be seen which have gained α-SMA expression (blue), while retaining E-cadherin expression (brown) (arrows), which is most clearly seen in the high-power insert. Some α-SMA expressing cells have become elongated and lost E-cadherin expression (V-shaped arrowheads). All tubular epithelial cells and normal GEC are stained for E-cadherin, but lack α-SMA expression (arrowheads). Sections (c–f) are from day 21 anti-GBM glomerulonephritis. (**c**) Strong staining for α-SMA (blue) is seen within a fibrocellular crescent with complete loss of E-cadherin (brown). Note that all tubular epithelial cells remained E-cadherin positive. (**d**) Double *in-situ* hybridization and immunostaining shwoing many elongated α-SMA-positive myofibroblasts (blue) within a cellular crescent which also exhibits strong TGF-β mRNA expression (purple). (**e**) *In-situ* hybridization showing strong FGF-2 mRNA expression (purple) by GPEC in an early glomerular crescent. (**f**) Triple immunostaining showing many elongated fibroblast-like cells within a fibrocellular crescent which express FGF-2 protein (brown) and PCNA (black). Note that some ED1+ macrophages (blue) within the crescent and glomerulus also show weak FGF-2 staining. Sections were counterstained with PAS (pink) (a–e). ×250 (a–c) and ×400 (d–f).

Some 25% of glomeruli at week 3 showed one or more GPEC with α-SMA staining, and this clearly preceded the development of crescent formation on week 5 (Figure 4a). The GPEC expressing α-SMA mRNA had an epithelial morphology and were attached to the Bowman's capsular basement membrane (CBM).

The specificity of the detection of α-SMA expression was confirmed by combined in situ hybridization and immunostaining (Figure 1c). De novo expression of α-SMA by GPEC was also observed in the early stages (day 7) of rat anti-GBM glomerulonephritis (Figure 2b), at the time when glomerular crescent formation was first detected (Figure 5a). Peri-

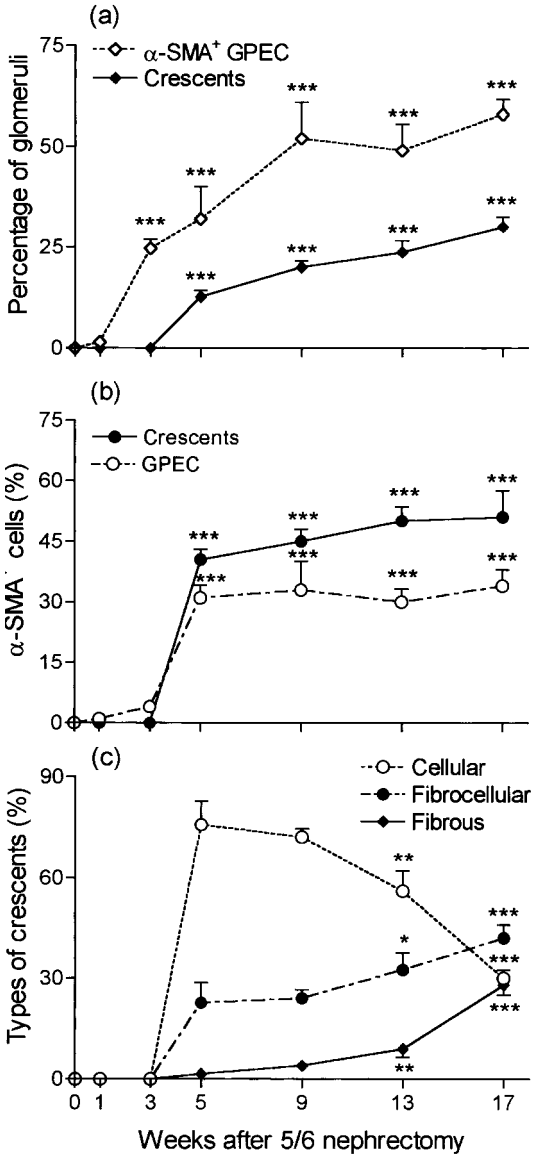

Fig. 4a–c. Quantitation of α-SMA immunostaining and glomerular crescent formation in the rat remnant kidney. (**a**) Graph showing the percentage of non-crescentic glomeruli containing one of more α-SMA-positive parietal epithelial cells (open diamonds, dashed line), and the percentage of crescentic glomeruli in which α-SMA-positive cells are present within the crescent (closed diamonds, solid line). (**b**) Graph shows the percentage of glomerular parietal epithelial cells (GPEC) expressing α-SMA in non-crescentic glomeruli (open circle, dashed line), and the percentage of crescent cells expressing α-SMA (closed circles, solid line). (**c**) Evolution of glomerular crescent formation. Glomerular crescents are divided into cellular (open circles, dotted line), fibrocellular (closed circles, dashed line), and fibrous phenotypes (closed diamonds, solid line). Each point represents the mean ± SEM for groups of 6 rats. $^{*}P<0.05$, $^{**}P<0.01$, $^{***}P<0.001$ *vs* normal animals (a,b) and *vs* week 5 animals (c) by ANOVA.

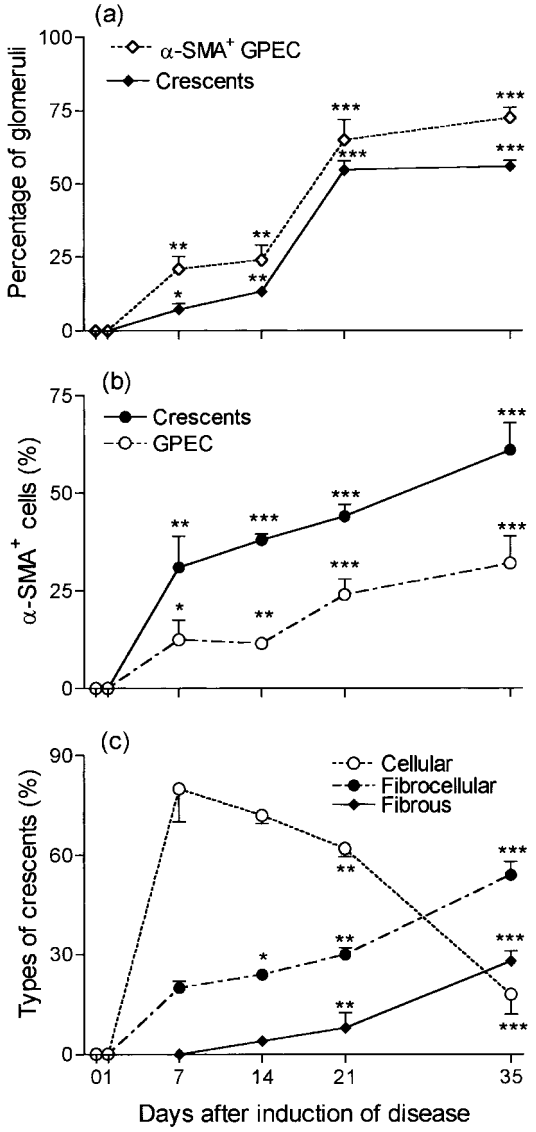

Fig. 5a–c. Quantitation of α-SMA immunostaining and glomerular crescent formation in rat anti-GBM glomerulonephritis. (**a**) Graph showing the percentage of non-crescentic glomeruli containing one or more α-SMA-positive parietal epithelial cells (open diamonds, dashed line), and the percentage of crescentic glomeruli in which α-SMA-positive cells are present within the crescent (closed diamonds, solid line). (**b**) Graph shows the percentage of glomerular parietal epithelial cells (GPEC) expressing α-SMA in non-crescentic glomeruli (open circle, dashed line), and the percentage of crescent cells expressing α-SMA (closed circles, solid line). (**c**) Evolution of glomerular crescent formation. Glomerular crescents are divided into cellular (open circles, dotted line), fibrocellular (closed circles, dashed line) and fibrous phenotypes (closed diamonds, solid line). Each point represents the mean ± SEM for groups of 6 rats. $^{*}P<0.05$, $^{**}P<0.01$, $^{***}P<0.001$ *vs* normal animals (a,b) and *vs* week 5 animals (c) for ANOVA.

glomerular α-SMA$^+$ myofibroblasts were also evident in the early stages of disease, although the CBM was largely intact at this time (Figure 2b).

Further phenotypic evidence of GEMT was provided by double immunostaining. Glomerular parietal epithelial cells in the early phase of transdi erentiation were stained positive for both α-SMA and the epithelial marker, E-cadherin (Figure 3b). Also evident were α-SMA$^+$ cells with an elongated morphology, spread along the CBM, which had lost E-cadherin expression (Figure 3b). Of note, partial disruption of the CBM was associated with *de novo* expression of α-SMA by GPEC in both disease models (Figure 1b,c and 2b).

One possible source of α-SMA$^+$ cells in crescent formation is the migration of 'activated' mesangial cells from the glomerular tuft. However, immunostaining using the OX-7 mAb, a mesangial cell marker, found no evidence of mesangial cells within cellular or fibrocellular crescents (data not shown).

The relationship between α-SMA expression by GPEC and the development of crescent formation is shown in Figures 4 and 5 and Table 1. The percentage of non-crescentic glomeruli containing GEPC with α-SMA staining increased steadily from 25% of glomeruli at week 3 to over 60% by week 17 in the remnant kidney (Figure 4a). This paralleled glomerular crescent formation (Figure 4a). A parallel relationship between the percentage of non-crescentic glomeruli with α-SMA staining of GEPC and glomerular crescent formation was also seen in rat anti-GBM glomerulonephritis (Figure 5a). When assessing all non-crescentic glomeruli, the percentage of GEPC expressing α-SMA gave a highly significant correlation with the absolute number of cellular, fibrocellular and fibrous crescents in both disease models (Table 1). In addition, the percentage of GEPC expressing α-SMA in all non-crescentic glomeruli gave a highly significant correlation with the number of α-SMA$^+$ cells in cellular, fibrocellular, and fibrous crescents (Table 1).

Ultrastructural identification of GEMT in the evolution of glomerular crescents

Using transmission electron microscopy, no actin microfilaments were observed in glomerular visceral or parietal epithelial cells in normal rats, sham-operated rats, or on day 1 of anti-GBM glomerulonephritis. Three weeks after 5/6 nephrectomy, characteristic actin microfilament bundles (stress fibres) with many dense bodies were seen in some GPEC in glomeruli with no crescent formation (Figure 6a). At this early stage of transformation, actin microfilaments lay in the basal side of the GPEC, parallel to the partially disrupted CBM (Figure 6a). These cells maintained a normal epithelial structure with apical–basal polarity and microvilli on the cell surface. Cells in the early stage of transformation had a large round or oval-shaped nucleus, and showed abundant cytoplasm and numerous mitochondria, consistent with proliferative activity as shown by PCNA expression.

A later stage in the transdi erentiation of GPEC was seen in fibrocellular crescents. Actin microfilaments with dense bodies became more abundant within transformed GPEC where Bowman's CBM remained partially intact (Figure 6b). In contrast to the basal localization of actin microfilaments in the early stage of transformation, actin microfilaments were formed in large bundles, lying parallel to the main axis of the cell and distributed through out the entire cytoplasm in GPEC in the late stage of transformation (Figure 6b). The apical–basal polarity, microvilli, and tight junctions were lost from these cells, and numerous vesicles within the cytoplasm were apparent (Figure 6b). Abundant collagen and characteristic myofibroblasts with peripheral microfilaments and well-developed endoplasmic reticulum were found within fibrocellular crescents (Figure 6b).

Myofibroblasts in the evolution of glomerular crescent formation

Most crescents present in the early stages of both disease models were of a cellular phenotype. With time, there was a progressive increase in the percentage of crescents with a fibrocellular or fibrous phenotype, and this was associated with an increase in the percentage of crescent cells expressing α-SMA (Figures 4b,c and 5b,c). In both disease models, α-SMA$^+$ cells were

Table 1. Correlation analysis of glomerular epithelial–myofibroblast transdi erentiation with glomerular crescent formation and progression in rat remnant kidney and anti-GBM glomerulonephritis

Cell population	Disease	All crescents α-SMA$^+$	Cellular α-SMA$^+$	Fibrocellular α-SMA$^+$	Fibrous α-SMA$^+$	Cellular crescents	Fibrocellular crescents	Fibrous crescents
Percent α-SMA$^+$ GEPC	Remnant kidney	0.856***	0.876***	0.775***	0.703***	0.759***	0.772***	0.548***
	Anti-GBM GN	0.708***	0.704***	0.632***	0.530**	0.810***	0.797***	0.645***
Percent α-SMA$^+$ cells in crescents	Remnant kidney	—	—	—	—	0.683***	0.896***	0.610***
	Anti-GBM GN	—	—	—	—	0.516**	0.869***	0.652***

Data pooled from all 5/6 nephrectomized animals ($n=36$) and pooled from all animals with anti-GBM glomerulonephritis (GN) animals ($n=30$). The percentage of glomerular parietal epithelial cells expressing α-SMA in non-crescentic glomeruli (per cent α-SMA$^+$ GEPC) and the percentage of glomerular crescent cells expressing α-SMA (per cent α-SMA$^+$ cells in crescents) (see Figures 4b and 5b) were correlated with the number of cellular, fibrocellular, and fibrous crescents and the number of α-SMA$^+$ cells within each of these crescent types using the Pearson correlation coe cient. Values shown are correlation coe cients. $^{**}P<0.1$, $^{***}P<0.001$.

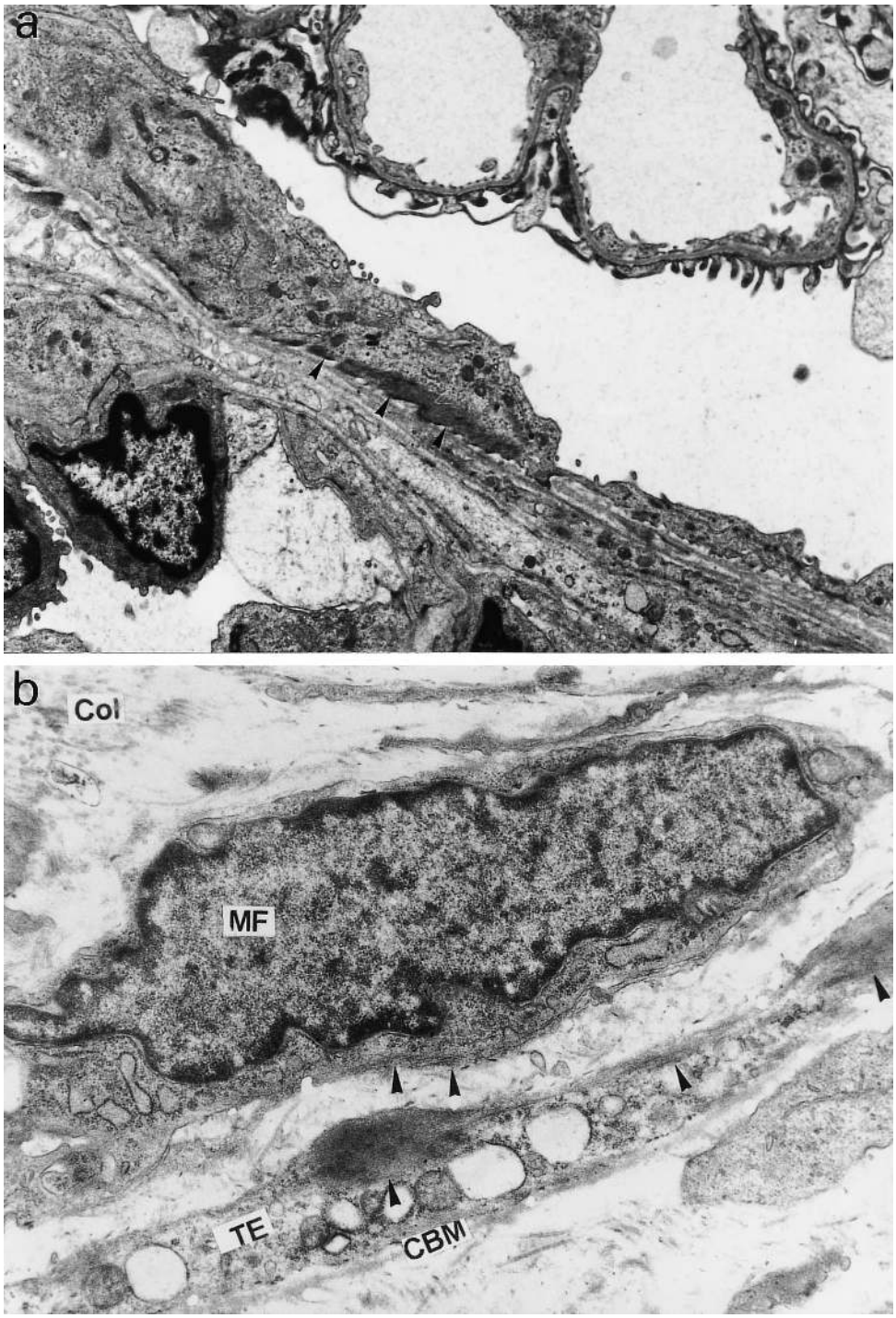

Fig. 6. Ultrastructural identification of glomerular epithelial–myofibroblast transdi erentiation. (**a**) Early GEMT at week 3 of the rat remnant kidney. A glomerular parietal epithelial cell contains characteristic actin microfilaments with many dense bodies (arrowheads) on the basal side of the epithelial peripheral cytoplasm, lying parallel to partially disrupted CBM. Note that the normal apical–basal polarity is maintained and some microvilli are observed. (**b**) A fibrocellular crescent at day 21 of rat anti-CBM glomerulonephritis. Ultrastructural identification of late stage GEMT shows a transformed glomerular parietal epithelial cell containing large bundles of actin microfilaments and dense bodies (arrowheads), many vesicles within the cytoplasm and a complete loss of epithelial polarity. Abundant collagen and characteristic myofibroblasts that contain peripheral microfilaments and rich reticulum endoplasm were also apparent. Col, collagen; CBM, capsular basement membrane; MF, myofibroblasts; TE, transformed epithelial cell. Magnification, (a) $\times 8000$, (b) $\times 12\,000$.

detected within cellular crescents (Figures 1d, 2c and 7), which accounted for 30–35% of total crescent cells. Fibrocellular crescents contained a large number of α-SMA$^+$ cells, approximately threefold more than in cellular crescents (Figure 7), and many of the α-SMA$^+$ cells showed an elongated morphology (Figures 1e and 2d,e). This increase in α-SMA$^+$ cells was associated with extensive disruption of the CBM. Indeed, α-SMA$^+$ cells accounted for 70–80% of total cells within fibrocellular crescents. However, more than 80% of the α-SMA$^+$ cells seen in fibrocellular crescents disappeared and were replaced by collagen in fibrous crescents (Figures 1f, 2f and 7).

The percentage of crescent cells expressing α-SMA$^+$ increased with time in both disease models (Figures 4b and 5b), and in both cases gave a significant correlation with the absolute number of cellular, fibrocellular, and fibrous crescents (Table 1).

Of note, double immunostaining showed that approximately 60% of α-SMA$^+$ cells within cellular and fibrocellular crescents were proliferating on the basis of PCNA expression (Figures 2c,e).

Expression of TGF-β1 and FGF-2 in the evolution of glomerular crescents

Weak expression of TGF-β1 and FGF-2 was seen in glomerular cells and GPEC in normal rat kidney by *in situ* hybridization and immunostaining (not shown).

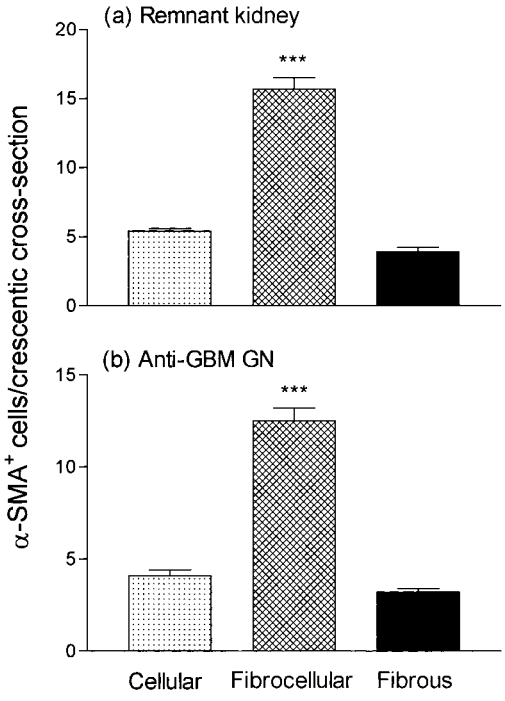

Fig. 7. Semi-quantitation of α-SMA expression within glomerular crescents in the rat remnant kidney and rat anti-GBM glomerulonephritis. (**a**) Remnant kidney; (**b**) Anti-GBM glomerulonephritis. Each bar represents the mean±SEM for groups for 20 rats with glomerular crescent formation. $^*P<0.05$, $^{**}P<0.01$, $^{***}P<0.001$ *vs* cellular and fibrous crescents.

There was a marked increase in both TGF-β1 and FGF-2 expression by GPEC in association with glomerular crescent formation (Figures 3d–f). Combined *in situ* hybridization and immunostaining showed that many elongated α-SMA$^+$ myofibroblasts in cellular and fibrocellular crescents expressed TGF-β1 mRNA (Figure 3d). Strong expression of FGF-2 mRNA by GPEC was evident in early cellular crescents (Figure 3e). The use of triple immunostaining showed that FGF-2 mRNA was expressed by many PCNA$^+$ elongated, fibroblast-like cells within fibrocellular crescents (Figure 3f). In addition, ED1$^+$ macrophages within fibrocellular crescents expressed FGF-2 protein (Figure 3f).

Discussion

The results of this study indicate that: (i) GEMT is an early event in the formation of cellular crescents; (ii) α-SMA$^+$ myofibroblasts are the major cell population in fibrocellular crescents; (iii) local proliferation is an important mechanism of myofibroblast accumulation within crescents; and (iv) local production of FGF-2 and TGF-β1 may contribute to local myofibroblast proliferation and GEMT respectively. The evidence for these conclusions is discussed below.

Prior to and during the early stages of crescent formation, parietal epithelial cells were found to express α-SMA mRNA and protein and lose expression of the epithelial marker, E-cadherin. These cells in the early stage of transdi erentiation were firmly attached to a largely intact CBM, and maintained a clear cuboidal epithelial morphology. This phenotypic evidence of GEMT was supported by ultrastructural studies showing actin microfilaments in GEPC that had a clear epithelial morphology and polarity. A late stage of transdi erentiation of GEPC was seen within cellular, and more particularly fibrocellular crescents, in which cells still adhering to the CBM lost apical-basal polarity, cell–cell junctions, became elongated, and showed large bundles of microfilaments and many dense bodies throughout the cytoplasm.

Cellular crescents consist of epithelial cells, macrophages, or a mixture of the two cell types. In addition, the current study has shown that α-SMA$^+$ myofibroblasts are also a component of cellular crescents. We postulate that the α-SMA myofibroblasts present in cellular crescents are derived from glomerular epithelial cells by transdi erentiation. This is supported by the temporal relationship between the appearance of α-SMA$^+$ GEPC in glomeruli prior to, or at the time of, the onset of glomerular crescent formation and the highly significant correlation between α-SMA$^+$ GPEC and the formation and evolution of glomerular crescents. Cellular crescents showed either no disruption, or local areas of partial disruption of the CBM, suggesting that the α-SMA$^+$ myofibroblasts in these crescents are derived by transdi erentiation and proliferation of glomerular cells, rather than by migration of periglomerular myofibroblasts into Bowman's space.

While it can be argued that α-SMA$^+$ myofibroblasts attached to the CBM are transdi erentiated parietal epithelial cells, it is possible that other α-SMA$^+$ myofibroblasts within cellular crescents (i.e. not attached to the CBM) could be transformed mesangial or visceral epithelial cells migrating from the glomerular tuft into Bowman's space.

The transdi erentiation described in the current study is not unique to glomerular parietal epithelial cells. Indeed, there are a number of defined circumstances under which epithelial cells can transdi erentiate into mesenchymal cells. For example, all kidney cells, except for the collecting duct cells, are derived from the metanephrogenic mesenchyme [30,31]. *In vitro*, suspension of definitive epithelia from a number of tissues, including tubular epithelial cell lines, in three-dimensional collagen type I gels promotes epithelial–mesenchymal transdi erentiation by turning o cytokeratin expression and turning on mesenchymal gene programs, inducing expression of fibroblast specific protein-1 [31–36]. In addition to phenotypic changes, transformed epithelial cells exhibit morphological changes such as a loss of cell–cell adhesion specialization and apical–basal polarity, and become elongated and very invasive with a new front end–back end mesenchymal polarity [31,36]. Similar morphological changes were observed in the current study.

Myofibroblasts were found to play an important role in the fibrous organization and progression of glomerular crescents, consistent with the importance given to α-SMA myofibroblasts in glomerulosclerosis and interstitial fibrosis [15–20]. There was a significant correlation between the number of α-SMA$^+$ cells and the progression of crescents from a cellular to a fibrocellular phenotype. The presence of many α-SMA$^+$ myofibroblasts in fibrocellular crescents is consistent with the active deposition of collagen leading to the development of acellular fibrous crescents. However, the origin of α-SMA$^+$ myofibroblasts in fibrocellular crescents remains uncertain. Some of these α-SMA$^+$ myofibroblasts may be derived by transdi erentiation of glomerular cells, but they may also arise from migration of periglomerular myofibroblasts into Bowman's space through the extensively ruptured CBM evident in fibrocellular crescents. In either case, the high levels of PCNA expression in the α-SMA$^+$ cells indicate that local myofibroblast proliferation is an important mechanism in their accumulation within Bowman's space. This is consistent with the high levels of α-SMA$^+$ myofibroblast proliferation described in experimental interstitial fibrosis [17,37].

Several possible mechanisms may promote the process of GEMT. First, TGF-β and fibroblast growth factors have been shown to induce synthesis of collagen types I, II, IV and V and FSP-1 by epithelial cell cells [32,38]. TGF-β and FGF-2 have also been shown to promote epithelial–mesenchymal transdi erentiation *in vitro* [39–43]. In the present study, marked upregulation of TGF-β1 and FGF-2 by glomerular cells was associated with GEMT and glomerular crescent formation and progression, consistent with a potential role of these growth factors in the transdi erentiation process and subsequent proliferation of myofibroblasts within crescents. The up-regulation of FGF-2 and TGF-β expression has previously been reported in these disease models [24,44]. Second, the association between localized partial disruption of the CBM and expression of α-SMA by GPEC suggests that direct interactions between the epithelial cells and the periglomerular extracellular matrix environment promotes induction of the transdi erentiation process. This is supported by *in vitro* studies showing that laminin A, a basement membrane component, plays a key role in initiating polarity of tubular epithelial cells [45]. Indeed, activation of the mesenchymal gene programme can be achieved in definitive epithelia by simple modifications of the extracellular matrix [31,35,36,46]. Therefore, partial disruption of the CBM allowing direct epithelial cell contact with the interstitial matrix may be crucial in the activation of the mesenchymal gene programme. This is consistent with our recent observation that disruption of the tubular basement membrane is associated with tubular epithelial–myofibroblast transdi erentiation in the development of interstitial fibrosis [47]. Third, the loss of epithelial cell adhesion molecule, E-cadherin, may also promote the transdi erentiation process. The addition of antibodies to E-cadherin causes disaggregation of the MDCK kidney epithelial cell line and their reversion to fibroblast-like cells [48,49]. Similarly, inhibition of E-cadherin expression by the use of anti-sense oligonucleotides causes epithelial cells to lose tight-junctions and became fibroblast-like [50]. Therefore, turning o expression of epithelial-specific genes is also required in the epithelial–mesenchymal transdi erentiation process. The present study showed that the gain of α-SMA expression by GPEC was associated with the loss of E-cadherin expression, providing *in vivo* evidence that the loss of adhesion molecules that maintain epithelial tight junctions is involved in the epithelial–myofibroblast transdi erentiation process.

A role for transdi erentiation in fibrogenesis has been described in a number of pathological situations. In liver fibrosis, lipocytes can transdi erentiate into myofibroblasts with expression of fibrogenic genes [51,52]. A similar transdi erentiation process has been described in pulmonary fibrogenesis [13]. We have also provided evidence that tubular epithelial cells are profibrogenic cells capable of transdi erentiation into α-SMA$^+$ myofibroblasts during the progression of tubulointerstitial fibrosis in rat remnant kidney model [47]. The present study extends these findings by: (i) providing more extensive phenotypic evidence for the process of epithelial–myofibroblast transdi erentiation in a pathological process, (ii) providing evidence that epithelial–myofibroblast transdi erentiation is an early event in a localized fibrotic process, and (iii) arguing that epithelial–myofibroblast transdi erentiation is of general importance in renal fibrosis, since the same transdi erentiation process was observed in both immune and non-immune models of crescentic glomerulonephritis.

In summary, this study provides, for the first time, evidence that glomerular epithelial–myofibroblast transdi erentiation participates in the development and progression of crescent formation. This process, which may in part be promoted by local production of TGF-β and FGF-2, provides a new approach to understanding the mechanisms of glomerular crescent formation and evolution.

Acknowledgements. We acknowledge the expert assistance of Miss W. Hong and Mr Z. P. Chen in the animal studies. This work was supported by grants from the National Science Council of Taiwan (86/87–2314-B075–062/048); Veterans General Hospital of Taiwan (86–259), National Health and Medical Research Council of Australia (960106), and Australian Kidney Foundation (G13N/98).

References

1. Kerr PG, Lan HY, Atkins RC. Rapidly progressive glomerulonephritis. In: Schrier RW, Gottschalk CW, ed. *Diseases of the Kidney.* Little, Brown and Co, Boston, 1996; 1619–1644
2. Cattell V, Jamieson SW. The origin of glomerular crescents in experimental nephrotoxic serum nephritis in the rabbit. *Lab Invest* 1978; 39: 584–590
3. Hancock WW, Atkins RC. Cellular composition of crescents in human rapidly progressive glomerulonephritis identified using monoclonal antibodies. *Am J Nephrol* 1984; 4: 177–181
4. Magil AB. Histogenesis of glomerular crescents: immunohistochemical demonstration of cytokeratin in crescent cells. *Am J Pathol* 1985; 120: 222–229
5. Boucher A, Droz D, Adafer E, Noel LH. Relationship between the integrity of Bowman's capsule and the composition of cellular crescents in human crescentic glomerulonephritis. *Lab Invest* 1987; 56: 526–533
6. Lan HY, Nikolic-Paterson DJ, Mu W, Atkins RC. Local macrophage proliferation in the pathogenesis of glomerular crescent formation in rat anti-glomerular basement membrane (GBM) glomerulonephritis. *Clin Exp Immunol* 1997; 110: 233–240
7. Ophascharoensuk V, Pippin JW, Gordon KL, Shankland SJ, Couser WG, Johnson RJ. Role of intrinsic renal cells versus infiltrating cells in glomerular crescent formation. *Kidney Int* 1998; 54: 416–425
8. Atkins RC, Nikolic-Paterson DJ, Song Q, Lan HY. Modulation of crescentic glomerulonephritis. *J Am Soc Nephrol* 1996; 7: 2271–2278
9. Morel-Maroger Striker L, Killen PD, Chi E, Striker GE. The composition of glomerulosclerosis. I. Studies in focal sclerosis, crescentic glomerulonephritis, and membranoproliferative glomerulonephritis. *Lab Invest* 1984; 51: 181–192
10. Silva FG, Hoyer JR, Pirani CL. Sequential studies of glomerular crescent formation in rats with antiglomerular basement membrane-induced glomerulonephritis and the role of coagulation factors. *Lab Invest* 1984; 51: 404–415
11. Lan HY, Nikolic-Paterson DJ, Atkins RC. Involvement of activated periglomerular leukocytes in the rupture of Bowman's capsule and glomerular crescent progression in experimental glomerulonephritis. *Lab Invest* 1992; 67: 743–751
12. Hogemann B, Gillessen A, Bocker W, Rauterberg J, Domschke W. Myofibroblast-like cells produce mRNA for type I and III procollagens in chronic active hepatitis. *Scand J Gastroenterol* 1993; 28: 591–594
13. Zhang K, Rekhter MD, Gordon D, Phan SH. Myofibroblasts and their role in lung collagen gene expression during pulmonary fibrosis. A combined immunohistochemical and *in situ* hybridization study. *Am J Pathol* 1994; 145: 114–125
14. Tang WW, Van GY, Qi M. Myofibroblast and α_1(III) collagen expression in experimental tubulointerstitial nephritis. *Kidney Int* 1997; 51: 926–931
15. Goumenos DS, Brown CB, Shortland J, El Nahas AM. Myofibroblasts, predictors of progression of mesangial IgA nephropathy? *Nephrol Dial Transplant* 1994; 9: 1418–1425
16. Hewitson TD, Becker GJ. Interstitial myofibroblasts in IgA glomerulonephritis. *Am J Nephrol* 1995; 15: 111–117
17. Hewitson TD, Wu HL, Becker GJ. Interstitial myofibroblasts in experimental renal infection and scarring. *Am J Nephrol* 1995; 15: 411–417
18. Zhang G, Moorhead PJ, El Nahas AM. Myofibroblasts and the progression of experimental glomerulonephritis. *Exp Nephrol* 1995; 3: 308–318
19. Roberts IS, Burrows C, Shanks JH, Venning M, McWilliam U. Interstitial myofibroblasts: predictors of progression in membranous nephropathy. *J Clin Pathol* 1997; 50: 123–127
20. Essawy M, Soylemezoglu O, Muchaneta-Kubara EC, Shortland J, Brown CB, El Nahas AM. Myofibroblasts and the progression of diabetic nephropathy. *Nephrol Dial Transplant* 1997; 12: 43–50
21. Kliem V, Johnson RJ, Alpers CE *et al.* Mechanisms involved in the pathogenesis of tubulointerstitial fibrosis in 5/6-nephrectomized rats. *Kidney Int* 1996; 49: 666–678
22. Lan HY, Paterson DJ, Atkins RC. Initiation and evolution of interstitial leukocytic infiltration in experimental glomerulonephritis. *Kidney Int* 1991; 40: 425–433
23. Dijkstra CD, Dopp EA, Joling P, Kraal G. The heterogeneity of mononuclear phagocytes in lymphoid organs: distinct macrophage subpopulations in the rat recognized by monoclonal antibodies ED1, ED2 and ED3. *Immunology* 1985; 54: 589–599
24. Mason DW, Williams AF. The kinetics of antibody binding to membrane antigens in solution and at the cell surface. *Biochem J.* 1980; 187: 1–20
25. Lan HY, Mu W, Nikolic-Paterson DJ, Atkins RC. A novel, simple, reliable, and sensitive method for multiple immunoenzyme staining: use of microwave oven heating to block antibody crossreactivity and retrieve antigens. *J Histochem Cytochem* 1995; 43: 97–102
26. Ng YY, Nikolic-Paterson DJ, Mu W, Atkins RC, Lan HY. Expression of basic fibroblast growth factor and its receptor in the progression of rat crescentic glomerulonephritis. *Nephrology* 1995; 1: 569–575
27. McHugh KM, Lessard JL. The nucleotide sequence of a rat vascular smooth muscle alpha-actin cDNA. *Nucleic Acids Res* 1988; 16: 4167
28. Qian SW, Kondaiah P, Roberts AB, Sporn MB. cDNA cloning by PCR of rat transforming growth factor beta-1. *Nucleic Acids Res* 1990; 18: 3059
29. Lan HY, Mu W, Ng YY, Nikolic-Paterson DJ, Atkins RC. A simple, reliable, and sensitive method of nonradioactive in situ hybridization: use of microwave heating to improve hybridization e ciency and preserve tissue morphology. *J Histochem Cytochem* 1996; 44: 281–287
30. Ekblom P, Weller A. Ontogeny of tubulointerstitial cells. *Kidney Int* 1991; 39: 394–400
31. Hay ED, Zuk A. Transformations between epithelium and mesenchyme: normal, pathological, and experimentally induced. *Am J Kidney Dis* 1995; 26: 678–690
32. Okada H, Dano TM, Kalluri R, Neilson EG. Early role of Fsp1 in epithelial–mesenchymal transformation. *Am J Physiol* 1997; 273: F563–574
33. Strutz F, Okada H, Lo CW *et al.* Identification and characterization of a fibroblast marker: FSPI. *J Cell Biol* 1995; 130: 393–405
34. Strutz F. Novel aspects of renal fibrogenesis. *Nephrol Dial Transplant* 1995; 10: 1526–1532
35. Zuk A, Hay ED. Expression of beta 1 integrins changes during transformation of avian lens epithelium to mesenchyme in collagen gels. *Dev Dyn* 1994; 201: 378–393
36. Zuk A, Matlin KS, Hay ED. Type I collagen gel induces Madin–Darby canine kidney cells to become fusiform in shape and lose apical–basal polarity. *J Cell Biol* 1989; 108: 903–919
37. Yang N, Wu LL, Nikolic-Paterson DJ *et al.* Local macrophage and myofibroblast proliferation in progressive renal injury in the rat remnant kidney. *Nephrol Dial Transplant* 1998; 13: 1967–1974
38. Creely JJ, DiMari SJ, Howe AM, Haralson MA. E ects of transforming growth factor-beta on collagen synthesis by normal rat kidney epithelial cells. *Am J Pathol* 1992; 140: 45–55

39. Jouanneau J, Gavrilovic J, Caruelle D *et al.* Secreted or non-secreted forms of acidic fibroblast growth factor produced by transfected epithelial cells influence cell morphology, motility, and invasive potential. *Proc Natl Acad Sci USA* 1991; 88: 2893–2897
40. Potts JD, Dagle JM, Walder JA, Weeks DL, Runyan RB. Epithelial-mesenchymal transformation of embryonic cardiac endothelial cells is inhibited by a modified antisense oligodeoxynucleotide to transforming growth factor beta 3. *Proc Natl Acad Sci USA* 1991; 88: 1516–1520
41. Sun D, Vanderburg CR, Odierna GS, Hay ED. TGFbeta3 promotes transformation of chicken palate medial edge epithelium to mesenchyme in vitro. *Development* 1998; 125: 95–105
42. Heikinheimo K, Happonen RP, Miettinen PJ, Ritvos O. Transforming growth factor beta 2 in epithelial di erentiation of developing teeth and odontogenic tumors. *J Clin Invest* 1993; 91: 1019–1027
43. Miettinen PJ, Ebner R, Lopez AR, Derynck R. TGF-beta induced transdi erentiation of mammary epithelial cells to mesenchymal cells: involvement of type I receptors. *J Cell Biol* 1994; 127: 2021–2036
44. Wu LL, Cox A, Roe CJ, Dziadek M, Cooper ME, Gilbert RE. Transforming growth factor beta 1 and renal injury following subtotal nephrectomy in the rat: role of the renin–angiotensin system. *Kidney Int* 1997; 51: 1553–1567
45. Klein G, Langegger M, Timpl R, Ekblom P. Role of laminin A chain in the development of epithelial cell polarity. *Cell* 1988; 55: 331–341
46. Boyer B, Thiery JP. Epithelium–mesenchyme interconversion as example of epithelial plasticity. *APMIS* 1993; 101: 257–268
47. Ng YY, Huang TP, Yang WC *et al.* Evidence for tubular epithelial–myofibroblast transdi erentiation in progressive tubulointerstitial fibrosis in 5/6 nephrectomized rats. *Kidney Int* 1998; 53: 864–876
48. Behrens J, Birchmeier W, Goodman SL. Dissociation of Madin–Darby canine kidney epithelial cells by the monoclonal antibody anti-Arc-1: Mechanistic aspects and identification of the antigen as a component related to uvomorulin. *J Cell Biol* 1985; 101: 1307–1315
49. Behrens J, Mareel MM, Van Roy FM, Birchmeier W. Dissecting tumor cells invasion: Epithelial cells acquire invasive properties after the loss of uvomorulin-mediated cell-cell adhesion. *J Cell Biol* 1989; 108: 2435–2447
50. Vleminckx K, Vakaet L, Mareel M, Fiers W, Van Roy F. Genetic manipulation of E-cadherin expression by epithelial tumor cells reveals an invasion suppressor role. *Cell* 1991; 66: 107–119
51. Gressner AM. Transdi erentiation of hepatic stellate cells (Ito cells) to myofibroblasts: a key event in hepatic fibrogenesis. *Kidney Int* 1996; 54 [Suppl]: S39–45
52. Tang L, Tanaka Y, Marumo F, Sato C. Phenotypic change in portal fibroblasts in biliary fibrosis. *Liver* 1994; 14: 76–84

Received for publication: 11.1.99
Accepted in revised form: 16.7.99